



## VISTA INTERNATIONAL JOURNAL ON ENERGY, ENVIRONMENT & ENGINEERING



### Debye Temperature and Elastic moduli of Cobalt ferrite nanoparticles prepared via Sol-Gel auto combustion method

**Rekha Parlikar<sup>1</sup>, Rani Dudhal<sup>2\*</sup>, Rahul Chilwar<sup>1</sup>, Vikas U. Magar<sup>2</sup> and K.M. Jadhav<sup>3</sup>**

<sup>1</sup>Yogeshwari Mahavidyalaya, Ambajogai, 431517, (M.S.) India

<sup>2</sup>Department of Physics, Deogiri College, Aurangabad -431005, Maharashtra, India

<sup>3</sup>Department of Physics, Dr. Babasaheb Ambedkar Marathwada University, Aurangabad – 431004, Maharashtra, India

**\*Corresponding author E-mail : vikasmagar3@gmail.com Mob.: +91-8888551733.**

#### ABSTRACT

In this work, nano-sized cobalt ferrite ( $\text{CoFe}_2\text{O}_4$ ) nanoparticles were synthesized via simple and cost-effective sol-gel auto-combustion method using citric acid as a fuel. The structural studies of fabricated fine cobalt ferrite nanoparticles were carried out by X-ray diffraction and Fourier transform infrared spectroscopy (FTIR) technique. Monophase formation with cubic spinel structure of the prepared cobalt ferrite nanoparticles was confirmed through X-ray diffraction analysis. The crystallite size was obtained through Debye-Scherrer formula which in nanoscale dimension. The lattice constant calculated using XRD data is in the reported range. The close examination to infrared spectrum shows the typical absorption bands in the range of 400  $\text{cm}^{-1}$  to 600  $\text{cm}^{-1}$  which confirms that, the presence of metal oxide stretching vibration is attributed to the formation of spinel ferrite nanoparticles. From this FTIR spectra, the various parameters such as, Debye temperature ( $\theta_D$ ), Force constant for tetrahedral ( $K_t$ ) and octahedral site ( $K_o$ ), Elastic stiffness constant ( $C_{ij}$ ), Stiffness constant ( $C_{il}$ ), Young's Modulus ( $Y$ ), Bulk Modulus ( $B$ ), Longitudinal elastic wave velocity ( $V_l$ ), Transverse elastic wave velocity ( $V_t$ ), Mean elastic velocity ( $V_m$ ), Rigidity modulus ( $R$ ) were calculated. All these elastic parameters are in the reported range.

**Keywords :** Cobalt ferrite, Sol-gel auto combustion, Debye temperature, Elastic moduli, Elastic wave velocities.

#### 1. Introduction:

Nanotechnology and Nanoscience is a widespread and interdisciplinary area of research and progress that has been growing explosively worldwide in the last decade. It has the potential for revolutionizing the traditions in which materials and products are created and the range and nature of functionalities that can be accessed. Nanomaterials are already having a significant commercial importance over the bulk material, which

will surely increase in upcoming years. Nanomaterials exhibit superior properties as compared to their bulk counterpart. The nanomaterials due to their smaller size exhibit large surface to volume ratio thereby they found many applications in various fields [1-3].

Among all the nanomaterials magnetic nanoparticles have received special attention over the last decade. These nanoparticles are widely used in memory devices [4], high-density magnetic recorders [5],

magnetocaloric applications [6], catalytic agents [7], magnetically driven drug delivery [8], hyperthermia [9], bio-sensors [10], bioactive molecule separation and magneto-optic devices [11].

In the range of several magnetic materials, ferrites are the important and widely used class of material. On the account of their significant structural, electrical and magnetic properties ferrites have applications in the field of antenna rods, transformer cores, memory devices, etc. The nanostructured ferrites have the several applications in the field of biomedicine, environment, automobile industry, sensors and actuators, catalytic applications, etc [12-14].

On the basis of crystal structure, ferrites are categorized into three main groups namely spinel, garnet, hexagonal and ortho ferrites. Each class of ferrites has its own significance and has applications in numerous fields. Among the various types of ferrite, spinel ferrites are the most important and broadly researched magnetic material. The spinel ferrites are unique materials exhibiting ferrimagnetic and semiconducting properties and can be considered as magnetic semiconductors.

Spinel ferrite nanoparticles produced by wet chemical method like sol-gel auto combustion with consistent size distributions are of great interest because of their unique magnetic properties, conquered by superparamagnetic [15]. Spinel ferrite nanoparticles can be used in biomedical applications. They are already in use for diagnostics for enhancement of contrast during NMR imaging and in detection of biomolecules by magnetic separation. Several new applications are developed also for therapeutics, for example in targeted drug delivery or in magnetic hyperthermia. One of the interesting applications of ferrites is in hyperthermia treatment which is considered as a supplementary treatment to chemotherapy [16]. The useful applications of these spinel ferrite nanoparticles are mainly due to their smaller size of the order of few nanometers.

Easy methods to tailor nanoparticles of desired size, shape, composition, purity, and physical properties are extremely important for practical

applications. Several synthesis methods have been developed to produce spinel ferrite nanoparticles, which include hydrothermal [17], solvothermal [18], mechanical milling [19], sol-gel [20], bacterial synthesis and so on. Most of them have been directed towards the preparation of particles, with a narrow size distribution in the range of few nanometers and more recently some approaches have been experimented with the idea of achieving assemblies with suitable sizes, in particular to meet the need of biomedical applications.

The important magnetic as well as electrical properties of spinel ferrites are responsive to a range of factors viz. synthesis techniques, variation in synthesis parameters, incorporation of dopants at interstitial sites, nature and amount of dopants etc [21-23]. The structural, electrical, dielectric and magnetic properties of spinel ferrite are more sensitive to the synthesis parameters compared to synthesis method and cation distribution. The synthesis parameters that affect the properties of final product are type of fuel, fuel to oxidizer ratio, amount of fuel percentage, ignition temperature, water content in precursor, pH of the solution, sintering temperature, sintering atmosphere etc [24].

## 2. Experimental method.

The sol-gel synthesis was based on the formation of a stable and homogenous solution made by dissolving a mixture of Cobalt (II) nitrate hexahydrate ( $\text{Co}(\text{NO}_3)_2 \cdot 6\text{H}_2\text{O}$ ,  $\geq 99\%$ , Fluka) and Iron (III) nitrate nonahydrate ( $\text{Fe}(\text{NO}_3)_3 \cdot 9\text{H}_2\text{O}$ ,  $\geq 98\%$ , Sigma-Aldrich) in water, which is a hydrolysis reaction. The solution was transformed into a sol and the gel by evaporation of the water, and during this time condensation reactions took place. Details of the whole preparation process are sketched in Fig.1 [28].

The precursors were used as received without any further purification. In order to maintain the homogeneity in both the sol and the gel during the condensation and other reactions, avoiding any precipitation or sedimentation of the products of the reactions, citric acid was employed as a chelating

agent. Both precursors were initially separately dispersed in de-ionized water for half an hour by stirring. Following this dispersion, the chelating agent was added and the mixture was left reacting under vigorous stirring for 2 h. Both solutions were then mixed together and left stirring for 24 h and after this the condensation reactions of both metal nitrates were allowed to take place. The quantity of each metal precursor was calculated so that the ratio of the two metals in the final material would be Co: Fe 1:2 and the quantity of citric acid was estimated assuming that each ferric ion would require two molecules of citric acid and each cobaltous ion would require two molecules of the chelating agent as well, so that the metal ions would be adequately chelated.

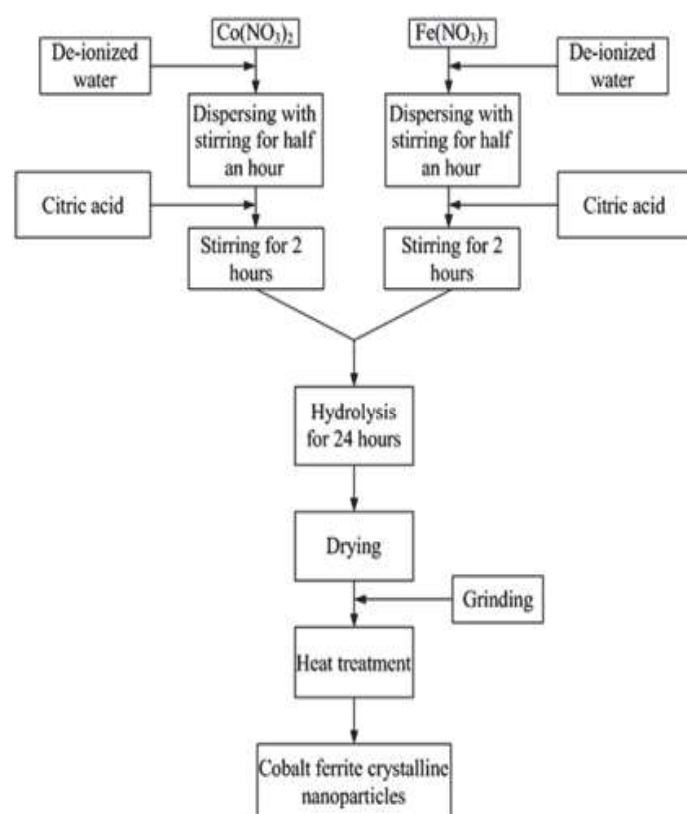


Fig. 1 Flow chart of cobalt ferrite nanoparticles preparation

### 3. Results and discussion

#### 3.1 Structural analysis of $\text{CoFe}_2\text{O}_4$

The structural characterization of the  $\text{CoFe}_2\text{O}_4$  nanoparticles was carried out by the unique XRD

technique. All the reflections obtained from XRD were indexed using Bragg's law. Fig. 2 shows the XRD pattern of  $\text{CoFe}_2\text{O}_4$  nanoparticles, in which reflections (220), (311), (222), (400), (422), (511), (440), (620), and (533) occurred which suggested the single-phase cubic spinel structure of prepared cobalt ferrite nanoparticles. The phase designing via sol-gel auto-combustion is dependent on several factors such as constituents, stirring time, stirring temperature, sintering temperature, type of fuel, and synthesis atmosphere, etc.

#### Lattice constant ( $a$ ) of $\text{CoFe}_2\text{O}_4$ nanoparticles

An average lattice constant ( $a$ ) for a cubic spinel structure of cobalt ferrite nanoparticles was calculated using the following relation;

$$a = d_{hkl} \sqrt{h^2 + k^2 + l^2} \quad (1)$$

Where  $d_{hkl}$  the interplanar spacing of two planes, ( $a$ ) is the lattice constant, and ( $hkl$ ) is the Miller indices of each plane. The calculated lattice constants ( $a$ ) of  $\text{CoFe}_2\text{O}_4$  nanoparticles were found from the XRD data is  $a = 8.3584 \text{ \AA}$  which is in good agreement with the other literature value. The value of the lattice parameter calculated using the above equations is presented in Table 1.

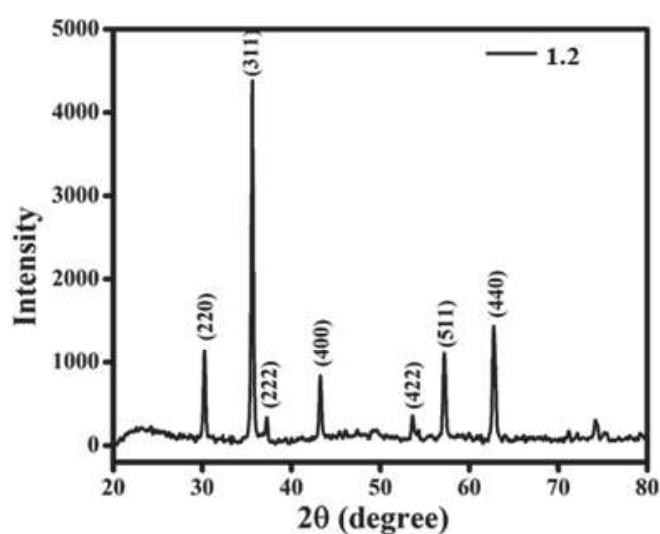


Fig.2 X-ray diffraction pattern of cobalt ferrite nanoparticles

**Table 1 Bragg's angle ( $2\theta$ ), interplanar spacing ( $d$ ), Miller indices of the plane ( $h,k,l$ ), lattice constant ( $a$ ) of cobalt ferrite nanoparticles**

$2\theta$	$\theta$	$\sin\theta$	$2\sin\theta$	$d$	$(a/d)^2$	$h$	$k$	$L$	$a$
30.245	15.1225	0.2609	0.5218	2.9519	8	2	2	0	8.3492
35.612	17.806	0.3058	0.6116	2.5183	11	3	1	1	8.3524
37.244	18.622	0.3193	0.6387	2.4116	12	2	2	2	8.3542
43.258	21.629	0.3686	0.7372	2.0892	16	4	0	0	8.3571
53.622	26.811	0.4511	0.9022	1.7073	24	4	2	2	8.3643
57.177	28.5885	0.4787	0.9571	1.6093	27	5	1	1	8.3625
62.736	31.368	0.5205	1.041	1.4794	32	4	4	0	8.3691
Average =									8.3584

### 3.2 FTIR analysis

Fourier transform infrared (FTIR) spectrum of the  $\text{CoFe}_2\text{O}_4$  nano- particles was recorded in the range of  $400\text{ cm}^{-1}$  to  $600\text{ cm}^{-1}$  as shown in Fig.3 The higher frequency band  $\nu_1$  between  $600\text{ cm}^{-1}$  and  $500\text{ cm}^{-1}$  is caused by the metal-oxygen bond (C=O) stretching at the tetrahedral site (A) and the lower frequency band  $\nu_2$  found in the range of  $450\text{ cm}^{-1}$  –  $380\text{ cm}^{-1}$  corresponds to the octahedral site (C O) stretching (B). These bands are known as the traditional spinel bands. According to Waldron's analysis, the force constant for tetrahedral ( $K_t$ ) and octahedral ( $K_o$ ) sites is,

$$K_t = 7.62 \times M_A \times \nu_1^2 \times 10^{-7} \quad (2)$$

$$K_o = 5.31 \times M_B \times \nu_2^2 \times 10^{-7} \quad (3)$$

$$K_{av} = \frac{K_t + K_o}{2} \quad (4)$$

where  $K_t$  and  $K_o$  are the force constants corresponding to tetrahedral and octahedral metal complexes.  $M_A$  is the mass of the tetrahedral site, while  $M_B$  is the mass of the octahedral site, and  $\nu_1$  and  $\nu_2$  are the frequencies of the tetrahedral and octahedral sites, i.e., 547 and 402.

The Debye temperature of  $\text{CoFe}_2\text{O}_4$  nanoparticles was calculated by following relation,

$$\theta_D = \frac{h\nu_{12}}{K_\beta} \quad (5)$$

where  $h$  is Planck's constant,  $c$  is the speed of light,  $K_\beta$  is the Boltzmann's constant, and  $\nu_{12}$  is the average wave number of absorptions. The elastic stiffness constant  $C_{ij}$  is calculated with the help of force constant as given by,

$$C_{ij} = \frac{K_{av}}{a} \quad (6)$$

where  $K_{av}$  is the average force constant and  $a$  is lattice constant (experimental). Stiffness constant  $C_{il}$  is calculated using elastic stiffness constant and Poisson's ratio as shown in,

$$C_{il} = \frac{\sigma \times C_{ij}}{1 - \sigma} \quad (7)$$

where  $C_{ij}$  is the elastic stiffness constant and  $\sigma$  is the Poisson's ratio (0.3227).

In order to measure the different elastic constants such as Young's modulus, bulk modulus, longitudinal elastic wave velocity, transverse elastic wave velocity and modulus of rigidity, their values are presented in Table 2.

The Young's modulus is shown as,

$$Y = \frac{(C_{ij} - C_{il})(C_{ij} + 2C_{il})}{C_{ij} + C_{il}} \quad (8)$$

where  $C_{ij}$  is the elastic stiffness and  $C_{il}$  is the stiffness constant.

The bulk modulus is presented by,

$$B = \frac{1}{3} [C_{ij} + C_{il}] \quad (9)$$

The longitudinal elastic wave velocity ( $V_l$ ) and transverse elastic wave velocity ( $V_t$ ) are given by,

$$V_l = \sqrt{\frac{C_{ij}}{\rho_x}} \quad (10)$$

$$V_t = \sqrt{\frac{C_{il}}{3\rho_x}} \quad (11)$$

where  $C_{ij}$  is the elastic stiffness constant and  $\rho_x$  is the X-ray density (5.3605).

Further, the calculated value of mean elastic wave velocity is explained as,

$$V_m = \left[ \frac{1}{3} \left( \frac{2}{V_l^3} + \frac{1}{V_t^3} \right) \right]^{-\frac{1}{3}} \quad (12)$$

where ( $V_l$ ) is the longitudinal elastic wave velocity and ( $V_t$ ) is the transverse elastic wave velocity.

The rigidity modulus can be calculated following relation,

$$R = \rho_x V_t^2 \quad (13)$$

where ( $\rho_x$ ) is the X-ray density (5.3605) and ( $V_t$ ) is the transverse elastic wave velocity.

Table-2 Calculated values of force constants ( $K_t$  and  $K_o$ ), avg. force constant ( $K_{avg.}$ ), Debye temperature ( $\theta_D$ ), elastic stiffness constant ( $C_{ij}$ ), stiffness constant ( $C_{il}$ ), Young's modulus ( $Y$ ), bulk modulus ( $B$ ), longitudinal wave velocity ( $V_l$ ), transverse wave velocity ( $V_t$ ), elastic wave velocity ( $V_m$ ), rigidity modulus ( $R$ ) for  $\text{CoFe}_2\text{O}_4$  nanoparticles.

Frequency Band ( $\text{cm}^{-1}$ )	v1	v2
	547	402
Lattice constant (a)	8.3584 ( $\text{\AA}$ )	
X-ray density ( $\rho_x$ )	5.3605 $\text{g/cm}^3$	
Force Constant ( $K_t$ )	$2.698 \times 10^2 \text{ N/m}$	
Force Constant ( $K_o$ )	$0.982 \times 10^2 \text{ N/m}$	
Avg. Force Constant ( $K_{avg.}$ )	$1.840 \times 10^2 \text{ N/m}$	
Debye temperature ( $\theta_D$ )	683.2 K	
Elastic stiffness constant ( $C_{ij}$ )	220 GPa	
Stiffness constant ( $C_{il}$ )	105.3 GPa	
Young modulus (Y)	151.95 GPa	
Bulk modulus (B)	108.5 GPa	
Longitudinal elastic wave velocity ( $V_l$ )	$6.417 \times 10^3 \text{ m/s}$	
transverse elastic wave velocity ( $V_t$ )	$3.705 \times 10^3 \text{ m/s}$	
Mean elastic wave velocity ( $V_m$ )	$2.134 \times 10^3 \text{ m/s}$	
Rigidity modulus (R)	73.3 GPa	

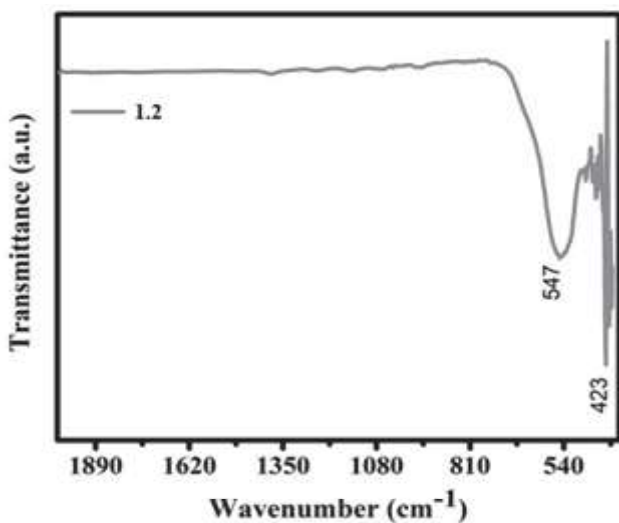


Fig.3 FT-IR spectra of cobalt ferrite nanoparticles

#### 4. Conclusion

$\text{CoFe}_2\text{O}_4$  nanoparticles are successfully fabricated by sol-gel auto-combustion method using citric acid as fuel. The processes of  $\text{CoFe}_2\text{O}_4$  development, as well as the characterization of the resulting compounds, were carried out with the help of X-ray diffraction, FTIR. The X-ray diffraction confirmed that the synthesized  $\text{CoFe}_2\text{O}_4$  nanoparticles belong to the inverse; single-phase; cubic spinel ferrite structure. The Miller indices ( $hkl$ ) plane reflections (220), (311), (222), (400), (422), (511), (440), (620) and (533) occurred in X-ray diffraction are in good agreement with the reported data. From the XRD data, we report the calculated lattice constant ( $a$ ) = 8.3584  $\text{\AA}$  for



CoFe<sub>2</sub>O<sub>4</sub> nanoparticles, which is significant as per the reported data in the referred literature. The crystallite size was calculated using the Debay-Sherrer's equation from the FWHM of intense (311) reflection in the XRD pattern. The crystallite size (*t*) of CoFe<sub>2</sub>O<sub>4</sub> nanoparticles has reported the achievement of nano-size was found to be 31.15 nm.

From FTIR analysis, Force Constant (*K<sub>t</sub>*)=2.698 × 10<sup>2</sup> N/m, Force Constant (*K<sub>o</sub>*)=0.982 × 10<sup>2</sup> N/m, Avg. Force Constant (*K<sub>avg.</sub>*) = 1.840 × 10<sup>2</sup> N/m, Debye temperature (*θ<sub>D</sub>*)=683.2 K.

Elastic stiffness constant (*C<sub>ij</sub>*)=220 GPa, Stiffness constant (*C<sub>il</sub>*)=105.3 GPa, Young modulus (*Y*) = 151.95 GPa, Bulk modulus (*B*) = 108.5 GPa, Longitudinal elastic wave velocity (*V<sub>l</sub>*) = 6.417 × 10<sup>3</sup> m/s, transverse elastic wave velocity (*V<sub>t</sub>*)=3.705 × 10<sup>3</sup> m/s Mean elastic wave velocity (*V<sub>m</sub>*) = 2.134 × 10<sup>3</sup> m/s, Rigidity modulus (*R*) = 73.3 GPa were calculated.

## References

- [1] Wilkinson, J. M. (2003) Nanotechnology applications in medicine. Medical device technology 14.5 (2003): 29-31.
- [2] Sunandan Baruah, Joydeep Datta (2009). Nanotechnology applications in pollution sensing and degradation in agriculture: a review. Environmental Chemistry Letters 7.3 (2009): 191-204.
- [3] Mamadou, Diallo, Jareemiah Duncon, Nora Savage, Nanotechnology applications for clean water. William Andrew Publishing, 2008.
- [4] M.T. Bohr, (2002) Nanotechnology goals and challenges for electronic applications, IEEE Transactions on Nanotechnology, 99 (2002) 56-62.
- [5] O. Kubo, T. Ido, H. Yokoyama, (1982), Properties of Ba ferrite particles for perpendicular magnetic recording media, IEEE Transactions on Magnetism, 18 (1982) 1122-1124.
- [6] P. Poddar, J. Gass, D.J. Rebar, S. Srinath, H. Srikanth, S.A. Morrison, (2006) Magnetocaloric effect in ferrite nanoparticles, Journal of magnetism and magnetic materials, 307 (2006) 227-231.
- [7] Sreekumar, K., and S. Sugunan. (2002) A comparison on the catalytic activity of Zn<sub>1-x</sub>CoxFe<sub>2</sub>O<sub>4</sub> (x= 0, 0.2, 0.5, 0.8 and 1.0) - type ferrosinels prepared via. a low temperature route for the alkylation of aniline and phenol using methanol as the alkylating agent. Applied Catalysis A: General 230.1-2 (2002): 245-251.
- [8] Sun, Conroy, Jerry S.H. Lec, Migin Zang (2008) Magnetic nanoparticles in MR imaging and drug delivery. Advanced drug delivery reviews 60.11 (2008): 1252-1265.
- [9] Pradhan, Pallab, Jyotsnendu Giri, Rinti Banarjee, Jayesh Bellare, Dharendra Bahadur, (2007) Preparation and characterization of manganese ferrite-based magnetic liposomes for hyperthermia treatment of cancer. Journal of Magnetism and Magnetic Materials 311.1 (2007): 208-215.
- [10] Yardımcı, Feyza S., Mehmet Senel, Abdulhadi Baykal (2012) Amperometric hydrogen peroxide biosensor based on cobalt ferrite-chitosan nanocomposite. Materials Science and Engineering: C 32.2 (2012): 269-275.
- [11] R. Grechishkin, M. Yu. Goosev, S.E. Ilyashenko, N.S. Neustroev, (1996), High-resolution sensitive magneto-optic ferrite-garnet films with planar anisotropy, Journal of magnetism and magnetic materials, 157 (1996) 305-306.
- [12] I. Sandu, Lionel Presmaners, Pierre Alphonse, Philippe Tailhades, (2006), Nanostructured cobalt manganese ferrite thin films for gas sensor application, Thin Solid Films, 495 (2006) 130-133.
- [13] C. Jagadish, Stephen Pearton (2011), Zinc oxide bulk, thin films and nanostructures: processing, properties, and applications, Elsevier, 2011.
- [14] M. Tomar, S.P. Singh, O. Parales, Perez, R.P. Guzman, E. Corderon, C. Rinaldi Romos (2005), Synthesis and magnetic behavior of nanostructured

- ferrites for spintronics, *Microelectronics journal*, 36 (2005) 475-479.
- [15] C. Liu, B. Bingsau zou, Adam Rondinore, Z. Jdin Zhang (2000), Reverse micelle synthesis and characterization of superparamagnetic MnFe<sub>2</sub>O<sub>4</sub> spinel ferrite nanocrystallites, *The Journal of Physical Chemistry B*, 104 (2000) 1141-1145.
- [16] A.K. Gupta, Mona Gupta (2005), Synthesis and surface engineering of iron oxide nanoparticles for biomedical applications, *Biomaterials*, 26 (2005) 3995-4021.
- [17] S. Komarneni, Maria Cristina D'Arrigo, Cristina (1998), Microwave hydrothermal synthesis of nanophase ferrites, *Journal of the American Ceramic Society*, 81 (1998) 3041-3043.
- [18] H. Wu, G. Liu, Xue Wang, Jiamin Zhang, Yuchen (2011), Solvothermal synthesis of cobalt ferrite nanoparticles loaded on multiwalled carbon nanotubes for magnetic resonance imaging and drug delivery, *Acta biomaterialia*, 7 (2011) 3496-3504.
- [19] S. Shenoy, P.A. Joy, M.R. Anantharaman (2004), Effect of mechanical milling on the structural, magnetic and dielectric properties of coprecipitated ultrafine zinc ferrite, *Journal of Magnetism and Magnetic Materials*, 269 (2004) 217-226.
- [20] S. Zahi, Mansur Hashim, A.R. Daud (2007), Synthesis, magnetic properties and microstructure of Ni-Zn ferrite by sol-gel technique, *Journal of Magnetism and Magnetic Materials*, 308 (2007) 177-182.
- [21] P.A. Shaikh, R.C. Kambale, A.V. Rao, Y.D. Kolekar (2010), Structural, magnetic and electrical properties of Co-Ni-Mn ferrites synthesized by co-precipitation method, *Journal of Alloys and Compounds*, 492 (2010) 590-596.
- [22] C.R. Vestal, and John Zhang (2003), Effects of surface coordination chemistry on the magnetic properties of MnFe<sub>2</sub>O<sub>4</sub> spinel ferrite nanoparticles, *Journal of the American Chemical Society*, 125 (2003) 9828-9833.
- [23] J. Nam, H.H. Jung, J.Y. Shin, J.H. Oh (1995), The effect of Cu substitution on the electrical and magnetic properties of NiZn ferrites, *IEEE Transactions on Magnetics*, 31 (1995) 3985-3987.
- [24] S. Ammar, J. Jouini, F. Fievet, O. Stephan, C. Marhic, (2004), Influence of the synthesis parameters on the cationic distribution of ZnFe<sub>2</sub>O<sub>4</sub> nanoparticles obtained by forced hydrolysis in polyol medium, *Journal of non-crystalline solids*, 345 (2004) 658-662.
- [25] A. Sutka & G. Mezinskis (2012), Sol-gel auto-combustion synthesis of spinel-type ferrite nanomaterials, *Frontiers of Materials Science*, (2012) 1-14.
- [26] M. Sugimoto (1999), The past, present, and future of ferrites, *Journal of the American Ceramic Society*, 82 (1999) 269-280.
- [27] S. Prasad, N.S. Gajbhiye (1998), Magnetic studies of nanosized nickel ferrite particles synthesized by the citrate precursor technique, *Journal of Alloys and Compounds*, 265 (1998) 87-92.
- [28] M. Sajjia, M. Oubaha, T. Prescott, A.G. Olabi (2010), Development of cobalt ferrite powder preparation employing the sol-gel technique and its structural characterization, *Journal of Alloys and Compounds* 506 (2010) 400-406.

